Metal-mesh based transparent electrodes using roll-to-sheet ultraviolet soft imprinting

Cheng-Hsin Chuang ✉, *Bo-Hsiang Chang, Jian-Ming Chen, Deng-Maw Lu*

Department of Mechanical Engineering, Southern Taiwan University of Science and Technology, Tainan 71005, Taiwan
✉ *E-mail: chchuang@stust.edu.tw*

Published in Micro & Nano Letters; Received on 12th May 2016; Revised on 21st June 2016; Accepted on 23rd June 2016

Transparent conductive electrodes (TCEs) possessing a combination of high optical transmission and good electrical conductivity find applications in numerous optoelectronic devices. A low cost fabrication of a fine metal-mesh structure on rigid (glass) and flexible (polyethylene terephthalate – PET) substrates as a promising and feasible approach for fulfilling large size TCE requirements is proposed. A roll-to-sheet ultraviolet imprinting protocol to transfer microtrench structures using a flexible Polydimethylsiloxane stamp is utilised. The conductive silver ink is filled into the microtrench structures by controlling the processing parameters which include pressure, scraping angle and speed. The metal-mesh based glass and PET substrates show a transmission of about 90%, while the electrical resistance is as low as 6 Ω/□. Thus, this method can be utilised as an economically viable alternative to doped indium oxide in TCE applications.

1. Introduction: Transparent conducting electrodes (TCEs) find use in many optoelectronic devices including solar cells, light emitting diodes (LEDs) and electronic displays owing to their unique material properties which allows for low resistance electrical contact to active layers while enabling light transmission. Doped metal oxide films, in particular tin doped indium oxide (ITO), have long been the material of choice for fabricating TCEs as it displays high transmittance (90%) at low sheet resistances (10 Ω/□). However, ITO suffers from several drawbacks which include high material costs due to indium scarcity, damage to organic substrates during vapour phase sputtering, low infrared transmittance and high brittleness which make it unsuitable for applications in flexible optoelectronic devices [1]. These problems have motivated research of new TCE materials, especially those that can be deposited using low cost solution based methods where the coating rate is significantly faster than sputtering while still achieving comparable transmittance and sheet resistance values of ITO.

Carbon based materials like carbon nanotubes [2], graphene [3] and conductive polymers [4] like poly(3,4-ethylenedioxythiophene) poly(styrene sulfonate) (PEDOT: PSS) have been proposed as next generation TCE materials. However, their conductivity is strongly dependent on the fabrication process and is currently insufficient for many optoelectronic devices like solar cells and LEDs. For example, while graphene has comparable optoelectronic properties to ITO when grown at elevated temperatures using high cost and low throughput vacuum deposition methods, solution processed graphene films often suffer from low conductivity due to the high contact resistance between graphene flakes. Another class of materials that has gained widespread popularity is based on thin films containing metal nanowire networks [5, 6]. In particular, solution based silver nanowire thin films have been explored because of their high conductivity, transparency, flexibility and low fabrication costs. However, they do suffer from drawbacks which include difficulty in obtaining a uniform nanowire distribution on the substrate, lower conductivity due to inherent defects as compared to bulk and a high junction resistance between nanowires. Recently, interconnected metallic mesh-type electrodes or metal grids have also been explored as promising alternatives as both their sheet resistance and their optical transmittance can be easily controlled by varying the grid width, spacing and thickness [7, 8]. Also they have the advantage of reduced junction resistance as compared to randomly aligned nanowire networks due to the formation of a continuous electrical pathway based on the metal grid lines crossing one another while the work function of the electrodes can be easily tuned by changing the metallic material used. Guo *et al.* pioneered the use of nanoimprint lithography to fabricate metal grids on various substrates and also showed their applicability for use in solar cells and LEDs [9, 10]. While printing technologies like inject, gravure, gravure offset and screen printing have been used to pattern metal grids directly for improved scalability, they are unable to achieve line widths less than 5 µm and this has been the major hindrance in the commercialisation of this technology.

In this Letter, we have used roll-to-sheet ultraviolet (UV) soft imprinting to pattern the interconnected mesh structure (line width <5 µm) on rigid and flexible substrates. In UV soft imprinting, a UV-curable liquid photopolymer is used instead of a thermoplastic polymer to coat the substrate while the stamp is made of a transparent and flexible soft elastomeric material. After a conformal contact is made between the stamp and the substrate, the convex line structures present in the stamp are imprinted into resist for the microtrench, which becomes solid after curing in UV light. UV soft imprinting is a promising alternative to conventional imprint lithography techniques and offers technical advantages related to alignment accuracy and the simultaneous imprinting of complex three-dimensional (3D) micro and nanostructures due to the absence of thermal heating cycles and high imprint pressures. The UV-imprinted substrates with microtrenches are then filled with silver nanoparticulate ink to create large area TCEs. We believe that this method can be used as a cost effective solution to meet industrial level TCE requirements of high throughput with the ability to pattern large area, non-ideal surfaces in a single parallel process.

2. Experimental: We use a four step procedure to fabricate the metal-mesh structure on glass and polyethylene terephthalate (PET) substrates as shown in Figs. 1*a–d*.

First, a standard photolithographic protocol is used to fabricate the mesh structure with a line width, spacing and depth of 5, 250 and 5 µm, respectively, on a silicon wafer which serves as the master. To create the flexible soft stamp, a 10:1 mixture of polydimethylsiloxane (PDMS) elastomer (Sylgard 184, Dow Corning) to cross-linker was prepared and degassed in vacuum to remove air

doi: 10.1049/mnl.2016.0284

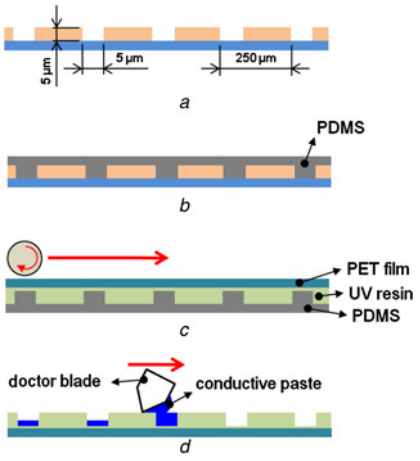

Fig. 1 *Fabrication process of metal mesh on glass substrate*
a Fabrication microtrench on wafer using photolithography
b Pattern transfer to PDMS mould
c UV curable pattern transfer by roll-to-sheet
d Conductive paste is filled into the microtrench structures by doctoring process

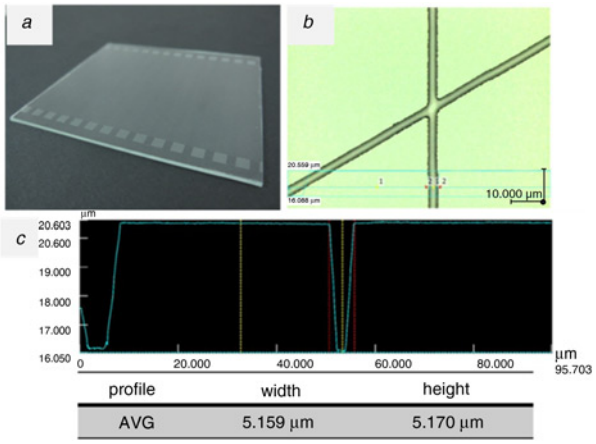

Fig. 3 *Physical dimensions of the patterned structures on glass substrate*
a Glass substrate with patterned metal-mesh structure transferred from PDMS stamp
b Microscopic image of patterned glass substrate
c Confocal microscopy analysis showing width and height of the metal-mesh structure on glass to be about 5 µm each

bubbles that formed during the mixing process. The liquid PDMS mixture was then cast on the silicon master and cured for 2 h at 90°C followed by the manual release to obtain the positive PDMS stamp. The stamp contains a patterned interconnected mesh structure protruding outwards and is a positive replication of the master. To perform UV imprinting, the substrate (glass or PET) was first coated with UV curable resin. Then, the patterned PDMS stamp is pressed onto the substrate using a roll-to-sheet protocol. This enables the imprinting of an interconnected mesh of microtrenches in the liquid resin followed by exposure to a UV light source that solidifies the resin due to cross linking. Finally, the soft PDMS stamp is released leaving the UV-cured resin with patterned microtrenches on the substrate. We then use an automated doctor blade scraping technique to fill the microtrenches with silver nanoparticulate ink (Ag ink). This is followed by baking in an oven at 130°C for 10 min for sintering of nanoparticles and solvent removal. We have investigated the influence of parameters like doctor blade angle and pressure on the height of

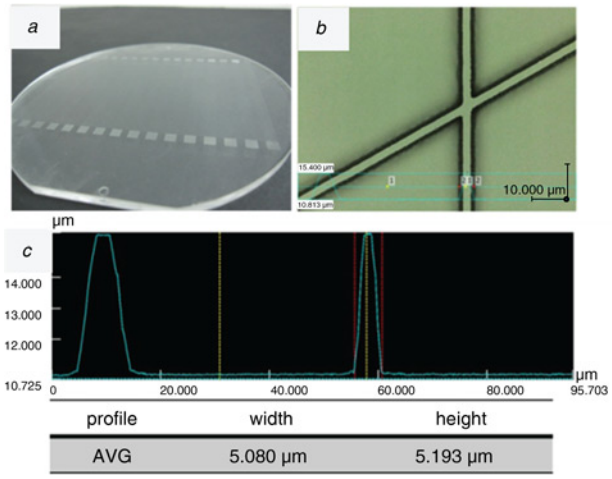

Fig. 2 *PDMS stamp*
a Image of the PDMS mould with an embedded metal-mesh structure transferred from a photolithographically patterned wafer
b Microscopic image of the PDMS mould
c Confocal microscopy analysis showing width and height of the metal-mesh structure on PDMS to be about 5 µm each

deposited Ag ink in the microtrenches and the scraping speed on the residual Ag ink left on the substrate surface. The optical transmission and haze of the metal-mesh coated glass and PET substrates are measured using a Haze meter (NDH-5000, Sun Great Technology Co. Ltd.). The sheet resistance is calculated using the equation $R = R_s\ (L/W)$ where R is the regular resistance (3D system) and can be calculated using a multimeter, R_s is the sheet resistance (2D system) and L and W correspond to the length and width of the metal-mesh electrode, respectively. Compared to two point resistance measurements obtained using a multimeter, four probe resistance measurements can be used to provide higher accuracy for calculating sheet resistance, especially when the observed resistance values are low. However, the line width and depth of the microtrench structure in which the Ag ink is deposited is 5 µm each while the tip of the probes has a diameter of about 700 µm. Furthermore, the deposited Ag ink using the scraping technique does not completely fill the microtrench structure to the top (height of Ag ink is <5 µm as shown in Fig. 5). This implies that the probe tip may not directly contact the deposited Ag unless a force is applied which can deform the resin to enable contact while there may be a further contact mismatch because the mesh has a crisscross pattern while the probes are arranged collinearly.

3. Results and discussion

3.1. PDMS stamp and UV-imprinted structures on rigid and flexible substrates: The flexible stamp used is the most critical element in UV imprinting and has a decisive effect in terms of resolution, uniformity and repeatability during imprinting. We have used confocal microscopy (VK-X200, Keyence, Japan) to ensure that the mesh pattern is successfully transferred from the master to the PDMS stamp. As shown in Figs. 2*a–c*, the PDMS stamp has an average line width and depth of 5 and 5 µm, respectively, and can thus be used to imprint microtrenches on PET and glass substrates.

The physical dimensions of the patterned structures on glass and PET substrates after roll-to-sheet UV imprinting using the PDMS stamp are shown in Figs. 3*a–c* and 4*a–c*, respectively. Confocal microscopy analysis of both substrates shows that the line width and depth of the imprinted microtrench structures is about 5 µm and this highlights the feasibility of using the PDMS stamp. The flexibility of the PDMS stamp as compared to stamps made of rigid materials ensures conformal contact at low pressures, even when used to imprint on flexible substrates. A further benefit is the ease of demoulding the PDMS from the substrate with an

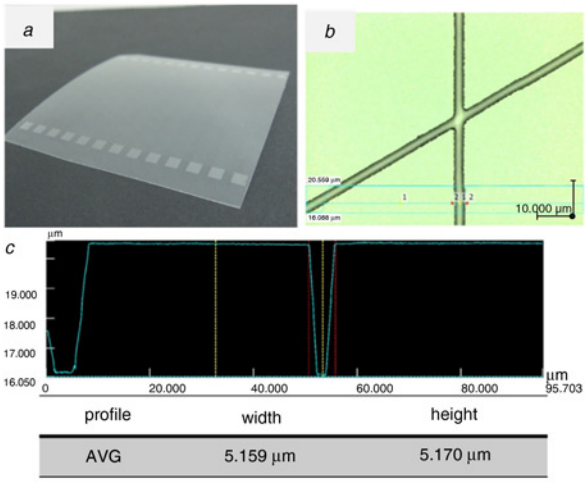

Fig. 4 *Physical dimensions of the patterned structures on PET substrate*
a PET substrate with patterned metal-mesh structure transferred from PDMS stamp
b Microscopic image of patterned PET substrate
c Confocal microscopy analysis showing width and height of the metal-mesh structure on PET to be about 5 µm each

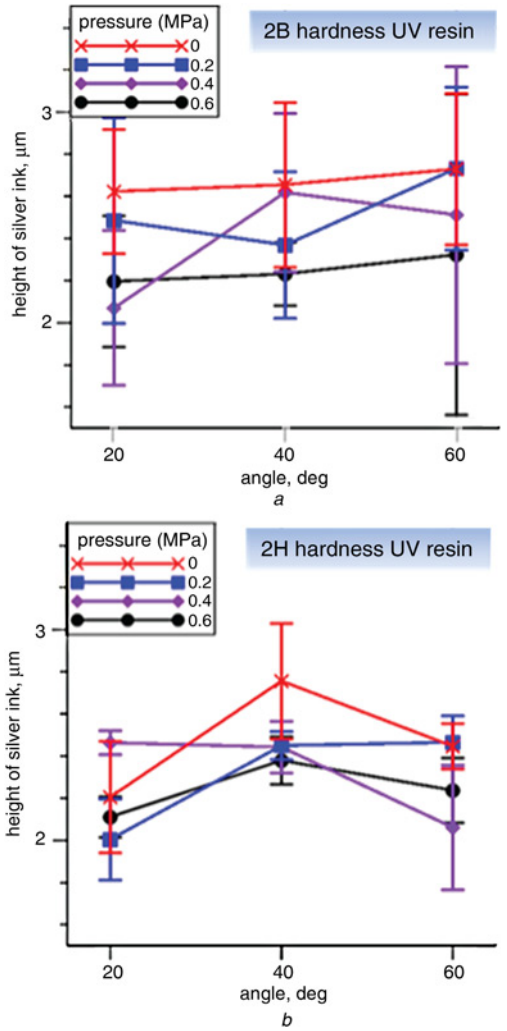

Fig. 5 *Dependence of the deposited Ag ink height on the doctor blade contact angle at different applied pressures for*
a 2B hardness resin
b 2H hardness resin

effectively smaller demoulding area and a lower release force. PDMS has been the most common choice for fabrication of soft stamps as it has attractive properties like low interfacial free energy, good chemical stability and high optical transparency.

3.2. Effect of pressure and scraping angle on the thickness of deposited Ag ink: The effect of different doctor blade contact angles (20°, 40°, 60°) and pressures (0–0.6 MPa) on the height of the deposited Ag ink for two kinds of UV resin used during UV imprinting on glass substrates are shown in Figs. 5*a* and *b*. The two UV resins differ based on their hardness values (2H > 2B). It was observed that the Ag ink thickness shows lesser variability for the harder resist (2H) as can be seen from the smaller error bars. In general, it was observed that the height of the Ag ink increases as the pressure decreases while the intermediate contact angle (40°) for the 2H resist showing maximum Ag ink deposition.

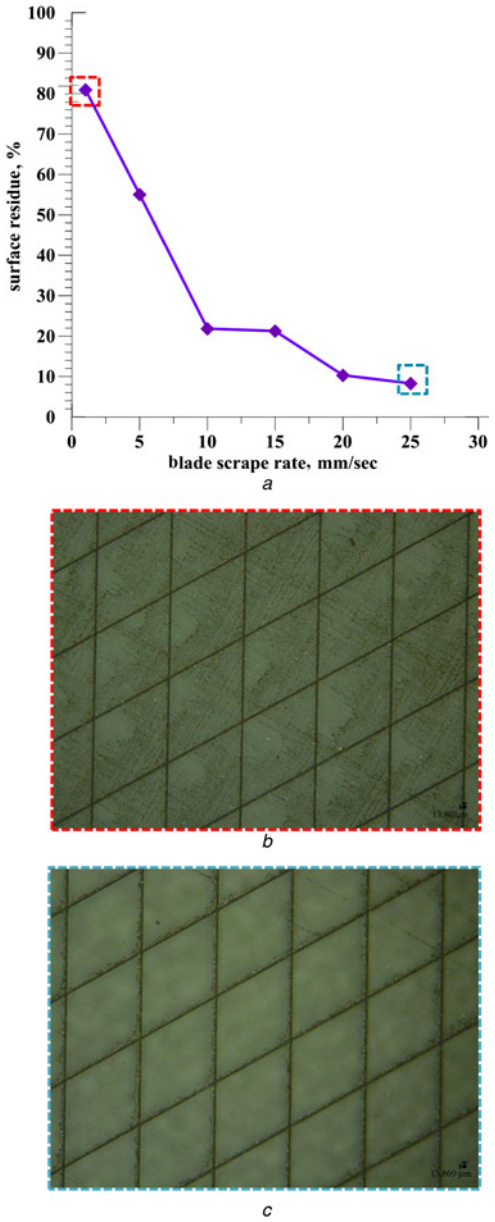

Fig. 6 *Images of the substrate surface using confocal microscopy*
a Effect of doctor blade scraping speed on the amount of residual Ag ink left on the substrate surface
Microscopic image showing residual Ag ink for scraping speeds of
b 2 mm/s
c 25 mm/s

doi: 10.1049/mnl.2016.0284

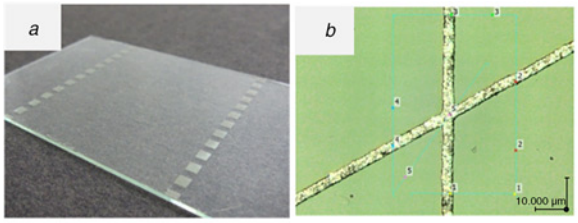

c

item	result
height of silver (µm)	3.6528
transmittance (%)	90.42
haze (%)	1.92
Sheet resistance (Ω/□)	6.12

Fig. 7 *Optoelectronic properties (transmittance, haze and sheet resistance) of the metal mesh containing glass substrate*
a Image of the transparent conductive glass substrate with the deposited Ag ink
b Optical microscopy image of the metal mesh on glass
c Characterisation results of the metal-mesh based glass

3.3. Effect of scraping speed on surface residual Ag ink: We analyse the effects of the scraping speeds (1, 5, 10, 15, 20 and 25 mm/s) on the residual Ag ink that is left behind on the substrate surface. The doctor blade contact angle and pressure is kept constant at 40° and 0.2 MPa, respectively, while a UV resin with hardness of 2H is used. After Ag ink deposition using the doctor blade technique, we obtain images of the substrate surface using confocal microscopy as shown in Fig. 6*a*. The white part in the image corresponds to the areas that are clean and do not contain any residual ink while the remaining areas on the substrate surface have residual ink. We have used a commercial graphics software (photoshop) to calculate the image pixels corresponding to the residual ink area and by comparing it to the total image pixels present, we can calculate the percentage of the surface containing residual ink. It was observed that more Ag ink remained on the surface as the scraping speed decreases as shown in Fig. 6*a*. This is because at lower speeds, the doctor blade experiences higher vibration while the opposite occurs at higher speeds.

3.4. Optoelectronic properties of metal-mesh based TCEs: The optoelectronic properties (transmittance, haze and sheet resistance)

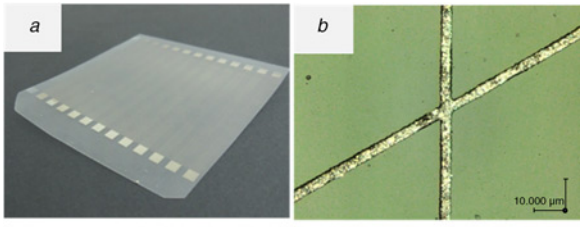

c

item	result
height of silver (µm)	3.6528
transmittance (%)	90.42
haze (%)	1.92
Sheet resistance (Ω/□)	6.12

Fig. 8 *Optoelectronic properties (transmittance, haze and sheet resistance) of the metal mesh containing PET substrate*
a Image of the transparent conductive PET substrate with the deposited Ag ink
b Optical microscopy image of the metal mesh on PET
c Characterisation results of the metal-mesh based PET

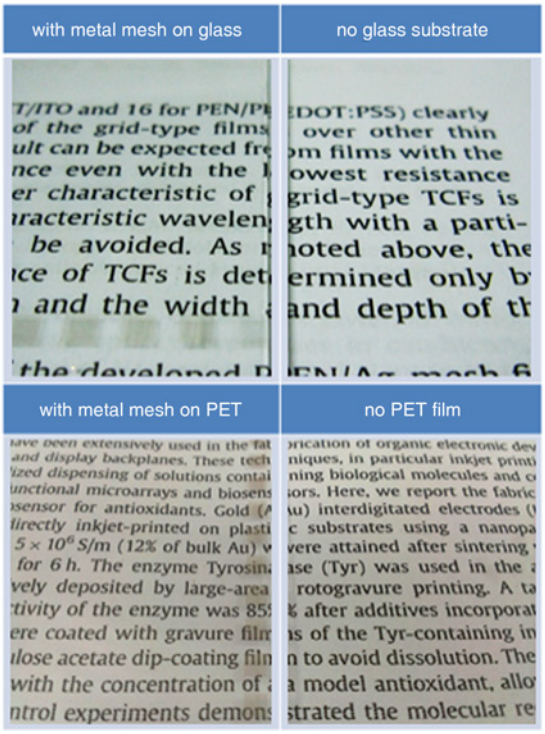

Fig. 9 *Observed optical transparency for metal-mesh based PET and glass substrates*

of the metal-mesh containing glass and PET substrates are shown in Figs. 7*a–c* and 8*a–c*, respectively. It can be seen that the transmittance (~90%) and sheet resistance (~6 Ω/□) is similar for both glass and PET substrates and is comparable to the optoelectronic properties of ITO. While the haze value for metal-mesh based glass (1.92%) is comparable to ITO (~1%), it is relatively larger for metal-mesh based PET (6.01%). The higher haze value obtained for PET as compared to glass can be attributed to the inherent higher optical transparency of glass relative to PET. The optical transparency of the metal-mesh based glass and PET substrates are further illustrated in Fig. 9 where it can be seen that the visibility of the underlying text is comparable to that in the absence of PET or glass. We have also shown that metal-mesh based PET films show good flexibility and durability as examined by bending the films repetitively over several hundreds of cycles without any obvious degradation in electrical conductivity as shown in Fig. 10. Thus, these highly conductive

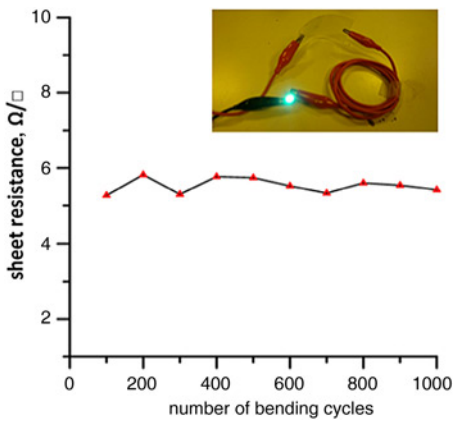

Fig. 10 *Testing the durability of the metal-mesh based PET films after several bending cycles*

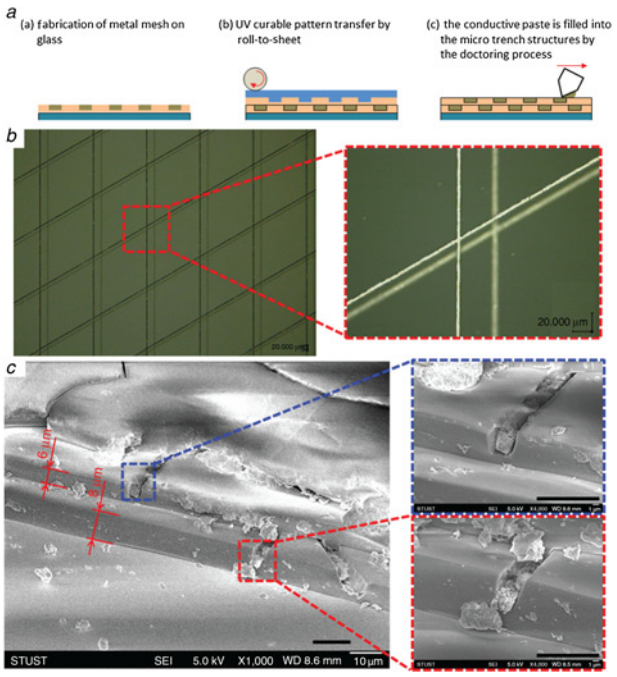

Fig. 11 *OGS technology*
a Schematic of fabrication protocol for double layer metal mesh on glass for OGS applications
b Optical microscopy
c SEM image of the fabricated double layer metal mesh (scale bar represents 10 µm)

and transparent electrodes on PET can find applications in emerging flexible optoelectronic devices.

3.5. Applicability for one glass solution (OGS) technology: OGS is an upcoming innovative touch screen technology that reduces the thickness of current capacitive touch panels by combining the touch panel and the protective glass into a single component. These thinner modules will result in improved optical properties and lower manufacturing costs due to reduction of components and easier implementation. We have shown the viability of obtaining patterned electrode layers separated by an insulating layer using a two-step Ω UV-imprinting protocol for OGS applications. The first step involves coating the glass substrate with UV resin (thickness of 8 µm as shown in the SEM image in Fig. 11*c*) followed by soft UV imprinting using a PDMS stamp and scraping Ag ink into the fabricated microtrenches as described in greater detail in Section 2. This is followed by coating a second layer of UV resin (thickness of 6 µm) and repeating the same protocol used to fabricate the first metal mesh. This results in two metal meshes separated by a thin insulating layer of UV resin. We believe that this is a scalable and cost effective strategy to fabricate large area OGS touch panels.

4. Conclusion: We have developed a simple, low cost and scalable method for the fabrication of large area conductive electrodes on flexible and rigid substrates based on an interconnected metal-mesh structure. The continuous electrical pathway achieved due to the ordered interconnected metal-mesh structure reduces junction resistance that is present in randomly aligned metal nanowire films with the ability to achieve conductivity values closer to the bulk. Furthermore, we believe that the roll-to-sheet UV-imprinting protocol used in this Letter can be scaled up to meet industrial production needs of TCEs with optoelectronic properties comparable to or even better than presently used doped metal oxide thin films.

5. Acknowledgment: This project was financially supported by Project for Developing the Model University of Science and Technology, MOE of Taiwan.

6 References

[1] Catrysse P.B., Fan S.: 'Nanopatterned metallic films for use as transparent conductive electrodes in optoelectronic devices', *Nano Lett.*, 2010, **10**, pp. 2944–2949
[2] Wu Z., Chen Z., Du X., *ET AL.*: 'Transparent, conductive carbon nanotube films', *Science*, 2004, **305**, pp. 1273–1276
[3] Wu J., Becerril H.A., Bao Z., *ET AL.*: 'Organic solar cells with solution-processed graphene transparent electrodes', *Appl. Phys. Lett.*, 2008, **92**, p. 263302
[4] Kim W., Makinen A., Nikolov N., *ET AL.*: 'Molecular organic light-emitting diodes using highly conducting polymers as anodes', *Appl. Phys. Lett.*, 2002, **80**, pp. 3844–3846
[5] Hu L., Kim H.S., Lee J.-Y., *ET AL.*: 'Scalable coating and properties of transparent, flexible, silver nanowire electrode', *ACS Nano*, 2010, **4**, pp. 2955–2963
[6] Sanchez-Iglesias A., Rivas-Murias B., Grzelczak M., *ET AL.*: 'Highly transparent and conductive films of densely aligned ultrathin Au nanowire monolayers', *Nano Lett.*, 2012, **12**, pp. 6066–6070
[7] Ho X., Lu H., Liu W., *ET AL.*: 'Electrical and optical properties of hybrid transparent electrodes that use metal grids and graphene films', *J. Mater. Res.*, 2013, **28**, pp. 620–626
[8] Hong S., Yeo J., Kim G., *ET AL.*: 'Nonvacuum, maskless fabrication of a flexible metal grid transparent conductor by low-temperature selective laser sintering of nanoparticle ink', *ACS Nano*, 2013, **7**, pp. 5024–5031
[9] Kang M.G., Guo L.J.: 'Nanoimprinted semitransparent metal electrodes and their application in organic light-emitting diodes', *Adv. Mater.*, 2007, **19**, pp. 1391–1396
[10] Kang M.G., Kim M.S., Kim J., *ET AL.*: 'Nanoimprint lithography: methods and material requirements', *Adv. Mater.*, 2008, **20**, pp. 4408–4413

doi: 10.1049/mnl.2016.0284